

Effects of Dissipation on Interchange Mode in Heliotron Plasma

ICHIGUCHI Katsuji*

National Institute for Fusion Science, 322-6 Oroshi-cho, Toki 509-5292, Japan

(Received: 18 January 2000 / Accepted: 21 April 2000)

Abstract

The stabilizing effects of the viscosity and heat conductivity on the interchange modes are studied numerically in a heliotron configuration. The viscosity cannot stabilize the mode completely although it reduces the growth rate substantially, while the heat conductivity can stabilize the mode completely. As substantial stabilizing effects are found in the range of the anomalous transport, they may explain the stable plasma observed in the Mercier unstable region in the CHS experiments.

Keywords:

heliotron, MHD, interchange mode, viscosity, heat conductivity

1. Introduction

For the steady state operation of the magnetically confined plasma, the MHD (magnetohydrodynamic) stability is necessary. In the Heliotron plasmas, the interchange mode is usually crucial because the confinement field is generated by the outer helical coils and there exist MHD equilibria without net toroidal current which is necessary in tokamaks. In some experiments of the CHS [1], the stable plasmas were observed at beta values above the Mercier limit [2]. These results indicate that there should be some stabilizing mechanism for the ideal and resistive interchange modes.

In the linear stability theory for the electrostatic model, it was analytically shown that the dissipation such as viscosity and heat conductivity have a stabilizing contribution against the interchange mode in Heliotron plasmas [3-5]. However, such stabilizing contribution in the electromagnetic model was not studied systematically. Thus, we consider the stabilizing effect of the viscosity and perpendicular heat conductivity against the global ideal and resistive MHD interchange mode. Particularly, in order to know

whether such dissipation should be a candidate of the stabilizing mechanism in the CHS and the LHD experiments, we focus on how much dissipation is needed to stabilize the modes.

2. Numerical Procedure

In order to study effects of the dissipation on the linear stability, the RESORM code [6] is utilized with adding the diffusion terms.

The RESORM code solves the reduced MHD equations based on the modified stellarator expansion method [7] for the poloidal magnetic flux Ψ , the stream function Φ and the plasma pressure P , which are given by

$$\frac{\partial \Psi}{\partial t} = - \left(\frac{R}{R_0} \right)^2 \mathbf{B} \cdot \nabla \Phi + \eta \nabla_{\perp}^2 \Psi, \quad (1)$$

$$\rho_m \frac{d \nabla_{\perp}^2 \Phi}{dt} = - \mathbf{B} \cdot \nabla \nabla_{\perp}^2 \Psi + R_0^2 \nabla \Omega \times \nabla P \cdot \nabla \zeta + \nu \nabla_{\perp}^4 \Phi, \quad (2)$$

and

$$\frac{dP}{dt} = \kappa \nabla_{\perp}^2 P. \quad (3)$$

*Corresponding author's e-mail: ichiguch@nifs.ac.jp

Here R and ζ denote the major radius and the toroidal angle, respectively, and the subscript 0 means the value at the magnetic axis. The averaged magnetic curvature, Ω , is given by

$$\Omega = \frac{1}{2\pi} \int_0^{2\pi} d\zeta \left(\frac{R}{R_0} \right)^2 \left(1 + \frac{|\mathbf{B} - \bar{\mathbf{B}}|^2}{B_0^2} \right) - 1, \quad (4)$$

where $\bar{\mathbf{B}}$ denotes the axisymmetric part of the magnetic field. The magnetic differential operator and the convective time derivative are defined as

$$\mathbf{B} \cdot \nabla = \frac{R_0 B_0}{R^2} \frac{\partial}{\partial \zeta} - \nabla \Psi \times \nabla \zeta \cdot \nabla \quad (5)$$

and

$$\frac{d}{dt} = \frac{\partial}{\partial t} + \mathbf{v}_\perp \cdot \nabla_\perp, \quad \mathbf{v}_\perp = \left(\frac{R}{R_0} \right)^2 \nabla \Phi \times \nabla \zeta, \quad (6)$$

respectively, and $\nabla_\perp \equiv \nabla - \nabla \zeta (\partial / \partial \zeta)$. η denotes the resistivity which is set to 0 for the ideal modes. The perpendicular diffusion type terms are added to the vorticity equation and the equation of state to investigate the viscosity (ν) and the heat conductivity (κ) effect.

The RESORM code finds the linear mode with the largest growth rate by following the time evolution of a perturbation. The full implicit method is employed for the time evolution. As for the spatial discretization, the central difference method is employed in the radial direction and the Fourier series are used in the poloidal and toroidal direction in the straight field-line coordinates (ρ, θ, ζ) , where ρ means the square root of the normalized poloidal flux. Since the toroidally averaged equilibrium quantities evaluated from the three-dimensional VMEC results [8], the toroidal mode number is specified and the poloidal mode coupling is taken into account. Therefore, the inversion of the block-tridiagonal matrix is carried out at each time step in the case without any dissipation terms.

If this scheme would be employed for the present problem, we would have to treat the inversion of the block-pentadiagonal matrix which needs much more computational region because the viscosity term involves the forth-order derivative in the radial direction. In order to avoid this situation, we modified the scheme by employing the Okamoto and Amano's (OA) method [9], which is second order accurate in the time step Δt . This method requires dividing the linearized three-field equations into following two parts. One part is the equations without the viscosity term given by

$$\frac{\partial \Psi}{\partial t} = - \left(\frac{\partial}{\partial \zeta} + \tau \frac{\partial}{\partial \theta} \right) \Phi + \frac{1}{S} \nabla_\perp^2 \Psi, \quad (7)$$

$$\begin{aligned} \frac{\partial \nabla_\perp^2 \Phi}{\partial t} = & - \left(\frac{\partial}{\partial \zeta} + \tau \frac{\partial}{\partial \theta} \right) \nabla_\perp^2 \Psi \\ & - \tau \left(\frac{\partial \Psi}{\partial \rho} \frac{1}{\rho} \frac{\partial J_{\zeta eq}}{\partial \theta} - \frac{\partial J_{\zeta eq}}{\partial \rho} \frac{1}{\rho} \frac{\partial \Psi}{\partial \theta} \right) \\ & + \frac{\beta_0}{2e} \tau \left(\frac{\partial \Omega}{\partial \rho} \frac{1}{\rho} \frac{\partial P}{\partial \theta} - \frac{\partial P}{\partial \rho} \frac{1}{\rho} \frac{\partial \Omega}{\partial \theta} \right), \end{aligned} \quad (8)$$

$$\frac{\partial P}{\partial t} = - \tau \frac{dP_{eq}}{d\rho} \frac{1}{\rho} \frac{\partial \Phi}{\partial \theta} + \kappa \nabla_\perp^2 P, \quad (9)$$

where S , β_0 , ε and τ denote the magnetic Reynolds number, the beta value at the magnetic axis, the inverse aspect ratio, and the rotational transform. The subscript of 'eq' denotes equilibrium quantities. The other part is the diffusion equation with the viscosity given by

$$\frac{\partial \Phi}{\partial t} = \nu \nabla_\perp^2 \Phi. \quad (10)$$

The length and the time are normalized with the minor radius of the plasma and the poloidal Alfvén time. According to the OA scheme, the results at $t = t_0 + \Delta t$ can be obtained from the initial values at $t = t_0$ with the following three steps. At first, we let the solution of (10) after $1/2 \Delta t$ with the initial condition $\Phi(t_0)$ be Φ_1 and let $\Psi_1 = \Psi(t_0)$ and $P_1 = P(t_0)$. Second, we let the solution of (7)-(9) after Δt with the initial condition Ψ_1 , Φ_1 and P_1 be Ψ_2 , Φ_2 and P_2 , respectively. At last, we obtain $\Phi(t + \Delta t)$, $\Psi(t + \Delta t)$ and $P(t + \Delta t)$ by setting the solution of (10) after $1/2 \Delta t$ with the initial condition Φ_2 as $\Phi(t + \Delta t)$ and setting $\Psi(t + \Delta t) = \Psi_2$ and $P(t + \Delta t) = P_2$. In this scheme, each step can be carried out with the inversion of a block-tridiagonal matrix only.

3. Stabilizing Effects on Interchange Mode

In order to investigate the effects of the dissipation on the stability against the interchange mode for the Heliotron plasmas, we choose the currentless LHD (Large Helical Device) [10] equilibrium with the pressure profile of $P = P_0(1 - s^2)^2$, where s and P_0 are the normalized toroidal flux and the pressure at the magnetic axis, respectively. This equilibrium is Mercier unstable for $\beta_0 \geq 1.5\%$ and the resistive interchange mode can be unstable even at beta values below the Mercier limit because of the magnetic hill. Thus, we studied the effects on the $n = 2$ ideal mode found at $\beta_0 = 5\%$ and the $n = 2$ resistive mode for $S = 10^6$ found at $\beta_0 = 1\%$. In the case without any dissipation, the growth rate normalized by the Alfvén time of the ideal mode is 3.525×10^{-2} of which the dominant component the mode is $m = 3$, and the growth rate of the resistive mode is 9.224×10^{-3} of which the dominant components are $m = 3$ and $m = 4$. The mode structure of the stream

function Φ of the resistive mode is plotted in Fig. 1, which shows a typical interchange mode structure. The structure of the pressure P of the mode is quite similar to that of Φ .

Figure 2 shows the dependence of the growth rate on the viscosity without the heat conductivity. Significant reduction of the growth rates is seen both for the ideal and the resistive modes. Particularly, the reduction is remarkable around $\nu \sim 10^{-5}$ which

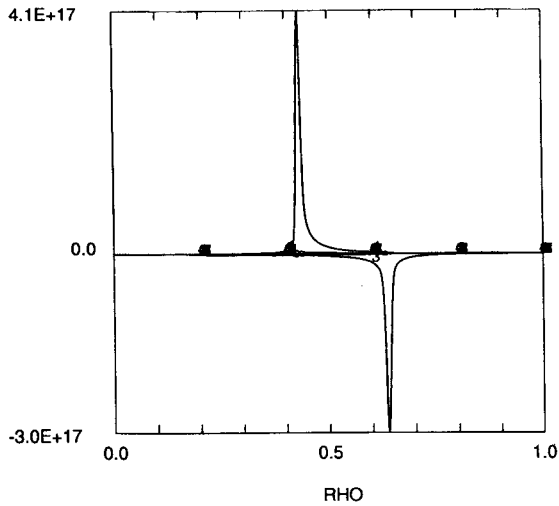


Fig. 1 Stream function of the $n = 2$ resistive interchange mode without any dissipation. The peaked profiles at $\rho = 0.43$ and 0.63 show the components of $m = 4$ and $m = 3$, respectively.

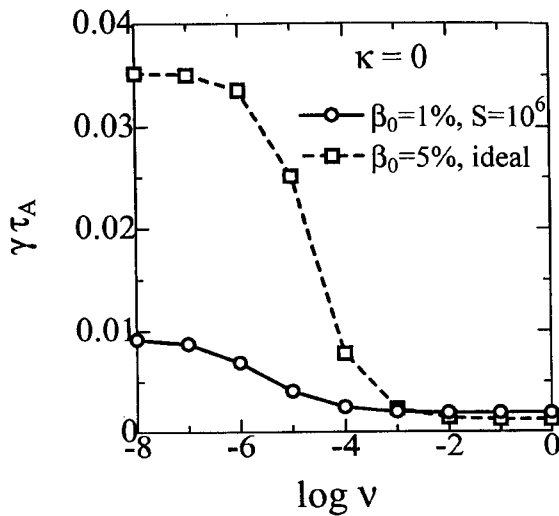


Fig. 2 Dependence of the growth rates on the viscosity for the resistive and the ideal interchange modes.

corresponds to $1 \text{ m}^2/\text{s}$ in the real dimension. This value is in the range of the anomalous transport observed in experiments in the heliotrons. However, either resistive or ideal mode cannot be stabilized completely by the viscosity only. Figure 3 shows the mode structure of the stream function of the resistive interchange mode for $\nu = 1$ and $\kappa = 0$. Comparing it with Fig. 1, the modes $m = 3$ and $m = 4$ are broader than those in the case without any dissipation. This is due to the diffusive effect of the viscosity term in the vorticity equation. The structure of the pressure is very similar to that without any dissipation.

Figure 4 shows the dependence of the growth rate on the heat conductivity without the viscosity. In this case, both the resistive and ideal modes can be completely stabilized by only the heat conductivity. It is noticed that substantial stabilizing effect is seen for the both modes in the range of the anomalous transport ($\kappa \sim 10^{-5}$) also in the case of the heat conductivity. There is a difficulty in obtaining the linear growth rate of the ideal mode near the stability limit with respect to κ because of bad numerical convergence. Figure 5 shows the structure of the perturbed pressure of the resistive interchange mode for $\nu = 0$ and $\kappa = 10^{-4}$. In this case, the diffusive effect of the heat conductivity term broadens the components of the pressure. The profile of the stream function is almost the same as that without any dissipations.

When we put both effects of the viscosity and the heat conductivity, both ideal and resistive interchange

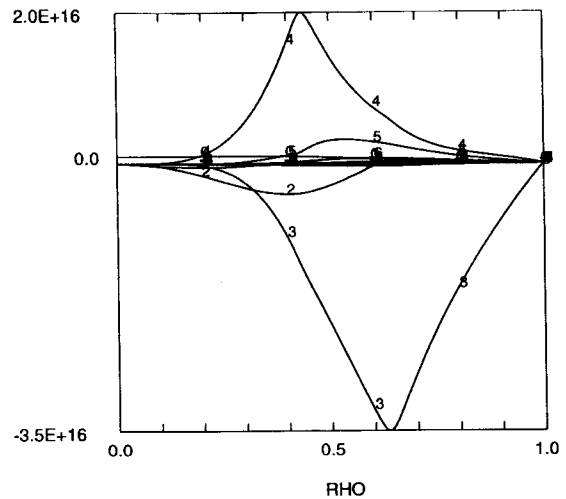


Fig. 3 Stream function of the $n = 2$ resistive interchange mode with $\nu = 1$ and $\kappa = 0$. Numbers show the poloidal mode numbers of the components.

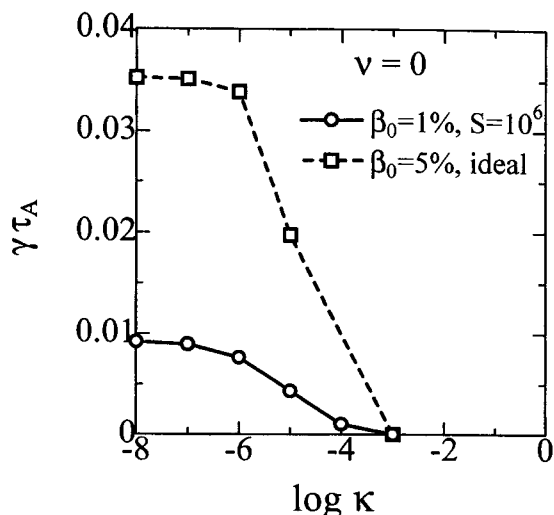


Fig. 4 Dependence of the growth rates on the heat conductivity for the resistive and the ideal interchange modes.

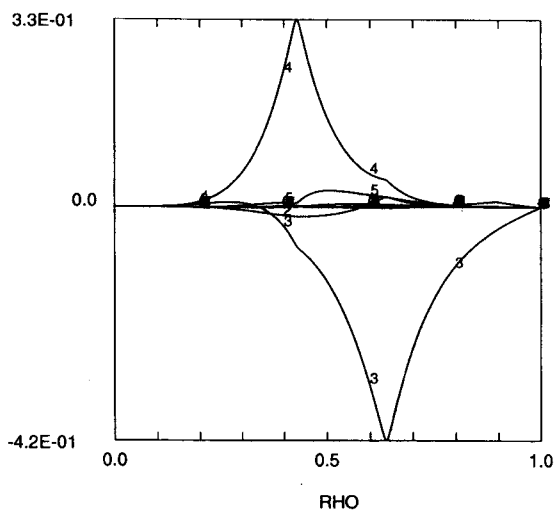


Fig. 5 Pressure of the $n = 2$ resistive interchange mode with $\nu = 0$ and $\kappa = 10^{-4}$.

modes are stabilized more effectively than in the case with one of the effects only. It was obtained, for example, that both ideal and resistive modes are completely stabilized at $\nu = 10^{-4}$ when the viscosity is varied with the heat conductivity fixed at $\kappa = 10^{-5}$.

4. Conclusions

In the present study, stabilizing effect of the viscosity and the heat conductivity in the perpendicular direction on both the ideal and the resistive interchange

modes in an LHD equilibrium is investigated by utilizing the reduced MHD equations. Substantial stabilizing effects of them in the range of the anomalous transport observed in experiments are found for both ideal and resistive modes. The viscosity cannot stabilize the modes completely although it reduces the growth rate significantly, while sufficient heat conductivity stabilizes the modes completely. When both effects are considered, the stabilizing contributions are almost superposed. Because of the diffusive model of the dissipation, the viscosity and the heat conductivity broaden the mode structures of the stream function and the pressure, respectively.

In the experiments in the CHS device, the plasmas are observed beyond the Mercier limit. The stabilizing effects of the dissipation in this study may be one of the candidate to explain such experimental results because the stabilizing range of the dissipation is realistic.

In the present study, we only keep the perpendicular component of the heat conductivity. The effect of the parallel heat conductivity and the model based on the neoclassical closure will be considered in the future study. Furthermore, the reason for the difficulty of the numerical convergence near the stability limit in the scan of the heat conductivity for the ideal mode will be worth examining analytically.

References

- [1] S. Okamura, K. Matsuoka, K. Nishimura *et al.*, Plasma Physics and Controlled Nuclear Fusion Research 1994, vol.1, (IAEA, Vienna) 381 (1995).
- [2] J.L. Johnson and J.M. Greene, Plasma Phys., **9**, 611 (1967).
- [3] B. Carreras, L. Garcia and P.H. Diamond, Phys. Fluids, **30**, 1388 (1987).
- [4] M. Yagi and M. Wakatani J. Phys. Soc. Jpn., **58**, 1624 (1989).
- [5] K. Itoh, K. Ichiguchi and S.-I. Itoh, Phys. Fluids, **B4**, 2929 (1992).
- [6] K. Ichiguchi, Y. Nakamura and M. Wakatani, Nucl. Fusion, **31**, 2073 (1991).
- [7] Y. Nakamura, K. Ichiguchi, M. Wakatani and J.L. Johnson, J. Phys. Soc. Jpn., **58**, 3157 (1989).
- [8] S.P. Hirshman, W.I. Van Rij and P. Merkel, Comp. Phys. Comm., **43**, 143 (1986).
- [9] M. Okamoto and T. Amano, J. Comp. Phys. **26**, 80 (1978).
- [10] A. Iiyoshi, A. Komori *et al.*, in Proc, IAEA Fusion Energy Conference, Yokohama, 1998, IAEA-CN-69.